

Observation of a subgap density of states in superconductor-normal metal bilayers in the Cooper limit

Zhenyi Long, M. D. Stewart, Jr., Taejoon Kouh,* and James M. Valles, Jr.†
Department of Physics, Brown University, Providence, RI 02912

(Dated: June 29, 2018)

We present transport and tunneling measurements of Pb-Ag bilayers with thicknesses, d_{Pb} and d_{Ag} , that are much less than the superconducting coherence length. The transition temperature, T_c , and energy gap, Δ , in the tunneling Density of States (DOS) decrease exponentially with d_{Ag} at fixed d_{Pb} . Simultaneously, a DOS that increases linearly from the Fermi energy grows and fills nearly 40% of the gap for $T_c \approx 0.1 T_{c,bulk}^{Pb}$. This behavior suggests that a growing fraction of quasiparticles decouple from the superconductor as $T_c \rightarrow 0$. The linear dependence is consistent with the quasiparticles becoming trapped on integrable trajectories in the metal layer.

Simple metallic phases have a finite resistance in the zero temperature limit and a nonzero Density Of electronic States (DOS) at the Fermi energy, E_F . In two dimensions (2D), however, the scaling theory of localization asserts that simple metallic phases do not exist [1]. Ultrathin films exhibit a continuously decreasing conductance with decreasing temperature in support of this assertion [2]. Nevertheless, there exist an increasing number of quasi-2D systems with metallic transport properties at low temperatures. These include 2D electron gases formed in semiconductor heterostructures, which appear to show an Insulator to Metal transition with electron density [3] and ultrathin films of metals balanced on the brink of a superconducting transition by disorder [4] or magnetic field [5, 6]. These metallic phases are probably not simple Fermi liquids and their existence depends on electron-electron interaction effects [3, 7]. Recently, two groups proposed that 2D arrays of superconducting islands immersed in a metal undergo a quantum superconductor to metal transition (SMT) with decreasing island concentration [8, 9]. The resulting metallic phase has non-Fermi liquid properties including a pseudogap and anomalous magnetoresistance [9].

Furthermore, theories of mesoscopic Superconductor-Normal metal (SN) structures have revealed mechanisms by which a finite DOS can appear within the energy gap of superconducting structures. These states, which give the DOS a hybrid superconductor-metal appearance, correspond to quasi-particles that become partially trapped in the N regions [10, 11, 12]. Mesoscopic spatial fluctuations in the local conductivity can give rise to “quasi-localized” states within the N region. These states appear within the gap, smearing the gap edge and creating a DOS down to E_F [10]. Within semi-classical models [11, 12, 13], the DOS depends on whether the dynamics in the N region is chaotic or integrable. Quasiparticles on ballistic, integrable trajectories can become quasi-trapped in N regions and contribute a subgap DOS that grows linearly from E_F .

We have conducted a series of experiments on ultrathin SN bilayers in an effort to observe the proposed SMT [8, 9] and its associated metallic phase. These bilayers

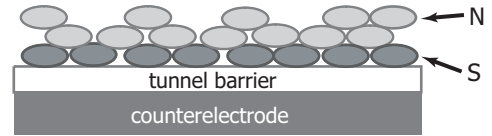


FIG. 1: Schematic cross section of the bilayer tunnel junction.

can be driven toward the metallic phase by increasing the metal layer thickness, d_N , at fixed superconductor thickness, d_S . Within quasiclassical proximity effect theories, the bilayers ought to have a hard, BCS gap in the DOS and make a transition to a metal phase only as $d_N \rightarrow \infty$. Contrary to this expectation, our previous work showed that their superconducting transition temperatures, T_c , decrease faster with d_N than quasi-classical predictions suggesting the approach to a SMT [14].

Here we present electron tunneling measurements showing that the DOS of ultrathin SN bilayers develops a hybrid superconductor-metal appearance that becomes more metallic as T_c decreases. Specifically, the superconducting gap of ultrathin Pb-Ag bilayers systematically fills with states as T_c is decreased by increasing the metal thickness, d_{Ag} at fixed superconductor thickness, d_{Pb} . The subgap DOS is finite at E_F and rises linearly with energy with a slope that increases with d_{Ag} . Recent theories suggest that these subgap states are quasiparticles that become decoupled from the superconductor for times longer than the superconducting coherence time [10, 11, 12, 13]. The linear dependence is consistent with semiclassical theories of quasiparticles becoming trapped on integrable trajectories [11, 12, 13].

For these studies, Pb/Ag bilayers with ultraclean Pb/Ag interfaces were fabricated and measured *in situ* using quench condensation techniques in the UHV environment of a dilution refrigerator cryostat [14]. The metals were thermally evaporated onto fire polished glass substrates held at 8 K. Au/Ge contact pads and oxidized Al counterelectrodes with a small amount of magnetic impurities to prevent them from superconducting were deposited prior to cryostat mounting. To form bilayers,

a thin < 6 nm, electrically discontinuous, Pb film was deposited first followed by, without breaking vacuum or warming, a series of Ag depositions (see Fig. 1). The latter drove the bilayer through an insulator to superconductor transition [15, 16]. This procedure yielded a series of bilayers with a single d_{Pb} and a range of d_{Ag} that were probed with the same, 1.25 mm^2 area, tunneling counterelectrode and barrier. The transport and tunneling measurements were performed using standard 4 terminal, low frequency AC techniques. Data acquired on a series of bilayers with $d_{Pb} = 4.0 \text{ nm}$ and $4.2 < d_{Ag} < 19.3 \text{ nm}$ are presented here. This data set is the most complete and systematic. It exhibits features that are similar to those of other series with $1.5 < d_{Pb} < 6.0 \text{ nm}$.

The normalized, superconducting bilayer DOS, $N_S(E)$, is obtained from the normalized differential conductance, G_j , of the tunnel junction[17]:

$$G_j = \frac{G_S}{G_N} = - \int_{-\infty}^{\infty} N_S(E) \frac{\partial f(E + eV)}{\partial (eV)} dE$$

where G_S and G_N are the differential conductances, dI/dV , in the superconducting and normal states, respectively. I is the tunnel current and V is the voltage across the junction. f is the Fermi function and E is the energy measured from E_F . At low temperatures, $T < 0.1 T_c$, $G_j \approx N_S(eV)$. In the Cooper limit [18, 19, 20], N_S is predicted to assume the BCS form, $N_S^{BCS}(E, \Delta) = \text{Re}(E/\sqrt{E^2 - \Delta^2})$ where Δ is the energy gap.

The evolution of the resistive transitions, $R(T)$ and tunneling conductances, G_j , of a bilayer series driven toward the metallic state is shown in Fig. 2. The transitions are sharp and T_c , defined as the temperature at which $R(T)$ is half its normal state value, drops exponentially with d_{Ag} (inset). The G_j , obtained at $T = 60 \text{ mK} \ll T_c$, qualitatively resemble the BCS form, exhibiting an energy gap structure consisting of symmetric peaks and a depression at low voltages (Fig. 2b). Within the gap region, however, G_j has an approximately linear voltage dependence and a finite value at zero voltage (Fig. 2c) rather than an exponentially small value. This subgap conductance grows with d_{Ag} and fills nearly 40% of the gap for the bilayer with $T_c = 0.67 \text{ K}$. In addition, the conductance peaks are shorter and broader than the BCS prediction.

Depositing Pb atop a bilayer to create a trilayer reverses the above evolution as shown in Fig. 3 for a bilayer with $d_{Pb} = 1.4 \text{ nm}$ and $d_{Ag} = 7.1 \text{ nm}$. It's G_j resembled that of the lower T_c bilayers in Fig. 2. Adding an upper Pb layer sharpened the peaks, increased the energy gap and reduced the slope and zero voltage bias value of G_j . A second Pb evaporation continued these trends. We hasten to note that the reduction in the subgap conductance induced by the upper Pb layer is a sign that the subgap conductance reflects an intrinsic feature of

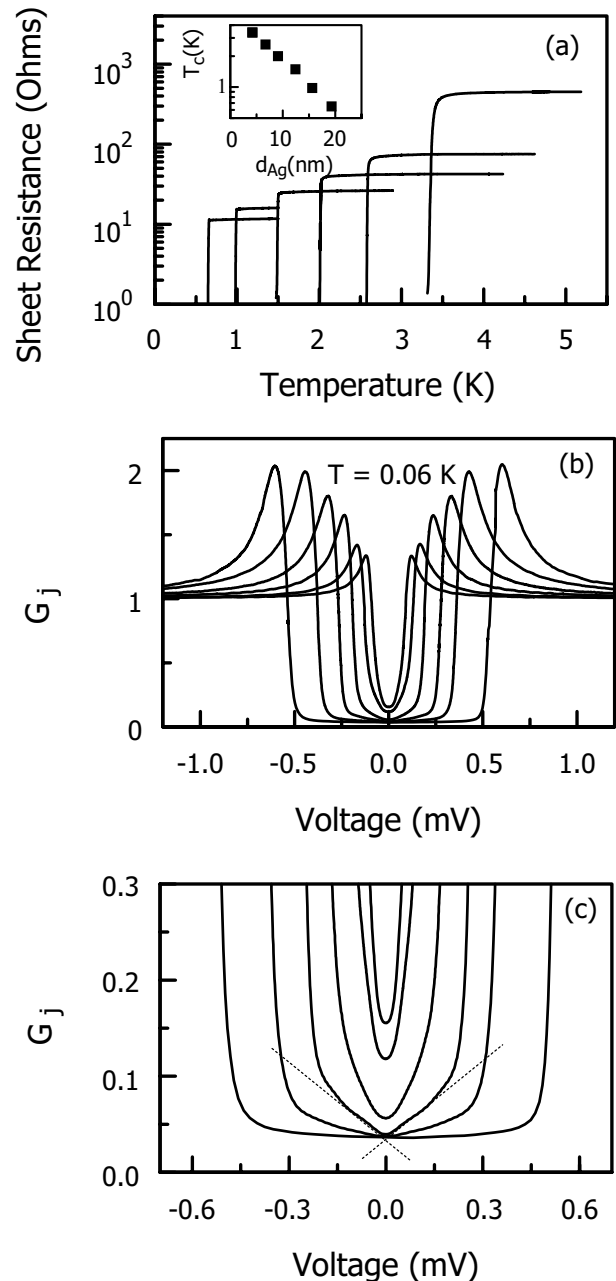


FIG. 2: (a) Sheet resistance vs. temperature for Pb/Ag bilayers with $d_{Pb} = 4 \text{ nm}$ and $d_{Ag} = 4.2, 6.7, 9.1, 12.4, 15.6, 19.3 \text{ nm}$. Inset: Semilog plot T_c vs. d_{Ag} . (b) G_j vs. V for the same bilayers. (c) Same data as in (b) on a finer voltage scale. The dashed lines are guides for the eye.

the DOS. A subgap conductance stemming from leakage would be unaffected by an upper Pb layer.

Except for the subgap conductance and the broadened conductance peaks, the data in Fig. 2 follow quasiclassical models of the proximity effect in the Cooper limit [18, 19, 20, 21]. In this limit, which applies to bilayers with $d_S, d_N \ll \xi$, the superconducting coherence length,

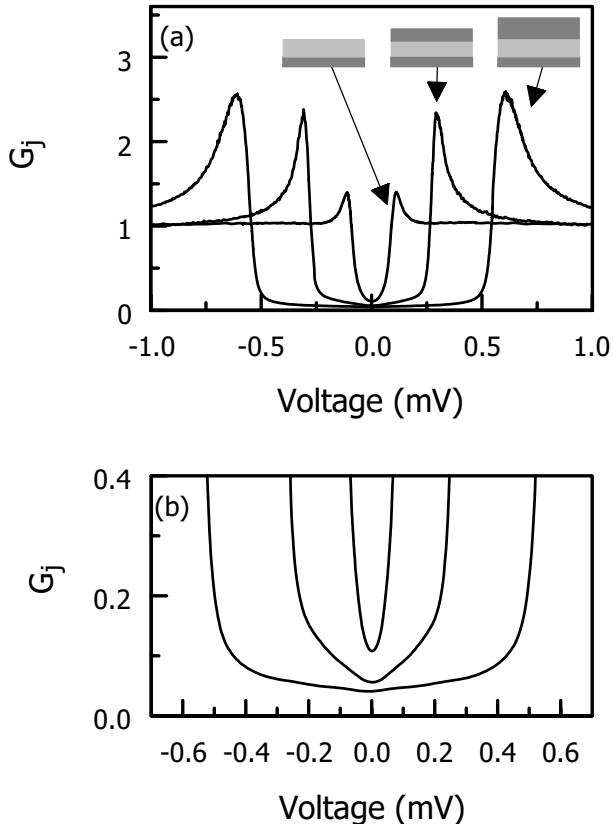


FIG. 3: (a) G_j at $T = 60$ mK vs. voltage for a bilayer $d_{Pb}/d_{Ag} = 1.4$ nm/7.1 nm, and two trilayers, $d_{Pb}/d_{Ag}/d_{Pb}$, of 1.4 nm/7.1 nm/2.2 nm and 1.4 nm/7.1 nm/5.4 nm. (b) Same data as in (a) on finer scales.

electrons near E_F pass back and forth between the S and N regions rapidly compared to Δ/\hbar . The effective superconducting coupling constant, $\lambda \propto \ln(T_c) \propto \ln(\Delta)$, is the volume average of the coupling constants in the N and S regions and thus, depends linearly on d_{Ag} in agreement with the inset of Fig. 2a [18]. The rapid motion renders the pairing amplitude uniform across the bilayer and thus, leads to a BCS form for the tunneling DOS [19] that roughly agrees with the data.

The extra breadth in the peaks can be attributed to the existence of a distribution of energy gaps in the bilayers. A distribution can naturally arise due to spatial variations in the film thickness ratio $x = d_{Ag}/d_{Pb}$ since $\Delta \propto T_c$ depends exponentially on x . Presuming $\Delta = \Delta_0 \exp(-kx)$, a (random) normal distribution of x yields a log-normal distribution for Δ and a broadened form of $N_S(E)$:

$$N_S^g(E, \bar{\Delta}) = \frac{1}{\sqrt{2\pi}k\sigma} \int_0^{\Delta_0} N_S^{BCS}(E, \Delta) \exp\left(-\frac{(\ln(\frac{\Delta}{\bar{\Delta}}))^2}{2(k\sigma)^2}\right) \frac{d\Delta}{\Delta}$$

where $\bar{\Delta}$ is the most probable energy gap and σ is the width of the x distribution. The parameters $\Delta_0 = 0.88$

meV and $k = 0.46$ were obtained by estimating Δ for each bilayer as the voltage at which $G_j = 1$ and fitting to the exponential form. Calculated G_j (see Fig. 4a) with broadened peaks that resemble the data require $\sigma < 25\%$ of x .

The states that systematically fill the superconducting gap, however, do not readily conform to a gap distribution model. The log-normal gap distribution drops too rapidly below $\bar{\Delta}$ to reproduce the linear DOS and finite zero bias conductance (see Fig. 4a). Creating the observed DOS at E_F would require that σ assume values at least 10 times larger than the values used to fit the peaks. Thus, we are led to the conclusion that the sub-gap DOS corresponds to quasiparticles that fall outside the Cooper limit picture and thus must relate to a new physical mechanism. A similar problem was encountered by Gupta and coworkers [22] who were unable to fit sub-gap structure in their STM data on Au/Nb films.

According to semi-classical theories, subgap states correspond to quasiparticles that propagate in an N region over distances more than ξ between successive Andreev scattering events with an NS interface [11, 12, 23, 24]. This situation normally occurs in SN structures with N region dimensions exceeding ξ , [24, 25, 26, 27, 28] or structures with integrable dynamics [11, 12], in which quasiparticles can execute nearly closed trajectories. Interestingly, the predicted DOS grows approximately linearly with energy for a variety of structures [11, 12, 13, 24]. In particular, Melsen and coworkers [11] proposed that for a rectangular integrable N billiard attached to a bulk S region, the distribution of path lengths, $P(L)$, between successive Andreev scattering events follows $P(L) \propto 1/L^3$ as $L \rightarrow \infty$. The normalized slope of the resulting linear DOS is $2/(\pi E_{Th})$ [11], where E_{Th} is the Thouless energy. Furthermore, the more general case of a mixed phase space that consists of both regular (integrable) and chaotic regions also yields a linear DOS and, in addition, a constant background DOS arising from phase space regions that are completely disconnected from the superconductor [13].

Guided by the above considerations and low temperature STM measurements showing that the bilayers consist of crystalline Pb and Ag grains [29, 30], we now assume that the bilayers present a mixed phase space of regular and chaotic regions [36]. Quasiparticles with chaotic trajectories contribute a BCS like portion, N_S^g , to the DOS while those with regular trajectories contribute a linear subgap DOS. Thus, we parameterize $N_S(E)$:

$$N_S(E) = \begin{cases} N_S^g(E, \bar{\Delta}) & \text{if } E > E_c \\ \alpha E + \beta & \text{if } E \leq E_c \end{cases}$$

where α and β are the slope and the intercept of the linear dependence, respectively, and E_c is the energy at which the two DOS intersect. Fig. 4a(right) shows G_j calculated from this DOS [37]. Fits to the data optimized to capture the subgap slopes and the peak heights

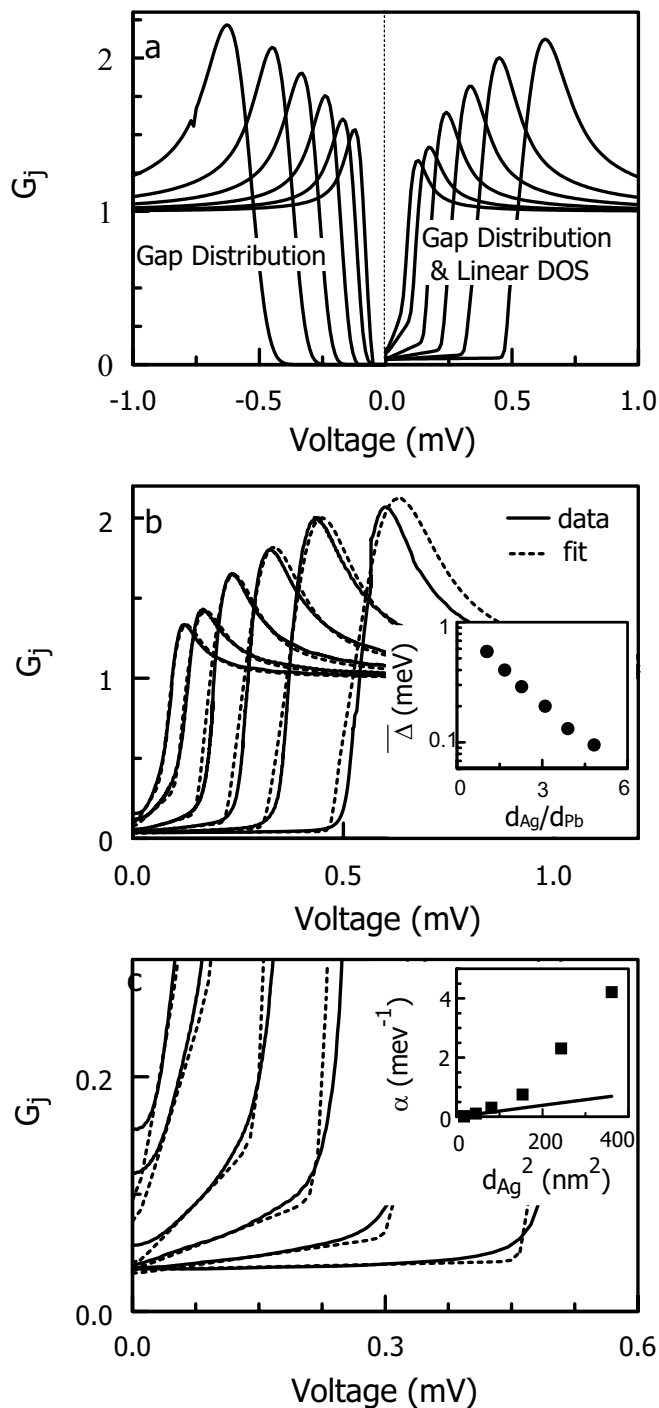


FIG. 4: (a) Comparison of G_j calculated using a log-normal gap distribution (left) and a log-normal distribution combined with a linear DOS within the gap (right). The corresponding curves have the same fitting parameters, $\overline{\Delta}$ and σ . (b) Data from Fig. 2a with fits. The fitting parameter $\sigma/(\frac{d_{Ag}}{d_{Pb}})$ decreases from 0.23 to 0.11 as d_{Ag} goes from 4.2 nm to 19.3 nm, while β increases from 0.033 to 0.065. Inset: Semilog plot of $\overline{\Delta}$, vs. d_{Ag}/d_{Pb} . (c) Same as (b) on finer scales. Inset: α vs. d_{Ag}^2 . The solid line gives the prediction based on transport measurements.

are shown in Fig. 4b and Fig. 4c. $\overline{\Delta}$ decreases exponentially with d_{Ag} (inset Fig. 4b) consistent with expectations for the Cooper limit. Since α is the slope of the DOS averaged over the regular phase space regions, α is proportional to the average $\overline{E_{Th}^{-1}}$. For these bilayers, we expect $\overline{E_{Th}^{-1}} \sim d_{Ag}^2/(\hbar D)$, where D is the intergrain diffusivity and thus $\alpha \propto d_{Ag}^2$. Fig. 4c compares the experimental α values with those estimated by $2d_{Ag}^2/(\pi\hbar D)$, using $D = 5 \times 10^{-3} m^2 s^{-1}$ as obtained from transport measurements. The two roughly agree at small d_{Ag} and deviate at higher d_{Ag} where the experimental α values grow more rapidly than expected. The deviation suggests that α also depends on T_c . This case has not been considered by the current theories [11, 13]. The trilayer data support this conjecture, exhibiting a reduction in α when T_c is increased at fixed d_{Ag} . Regardless, this deviation implies that the regular phase space regions occupy an increasing fraction of the total phase space volume as d_{Ag} increases. The concomitant increase of β implies a growing fraction of disconnected regions, as well. Consequently, as T_c decreases, a growing fraction of quasiparticles decouple from the S layer for times much greater than the superconducting coherence time.

Qualitatively, the growth in the subgap DOS gives the DOS a hybrid-metal-superconductor appearance that may be a sign of an approaching SMT. Ultrathin films near the disorder tuned superconductor-insulator transition exhibit a similar filling of the gap [31, 32] and low energy states have been invoked as a source of dissipation that drives the Quantum SMT observed in nanowires [33, 34, 35]. Perhaps these states arise due to similar quasiparticle trapping effects.

Tunneling experiments on ultrathin Pb-Ag bilayers at low reduced temperatures ($T/T_c < 0.1$) have revealed an unexpected linear DOS within their superconducting energy gap. The fraction of the gap filled with states grows with increasing d_{Ag} . We have identified the subgap states as quasiparticles that are weakly coupled to the superconductor layer. Within a semiclassical picture, these quasiparticles become trapped in regular regions of phase space.

The work was supported by nsf-dmr0203608. We acknowledge helpful conversations with Dmitri Feldman.

* Presently at: Aerospace and Mechanical Engineering Dept, Boston University, Boston, MA 02215.

† Electronic address: valles@physics.brown.edu

- [1] E. Abrahams *et al.*, Phys. Rev. Lett. **42**, 673 (1979).
- [2] G. Bergmann, Phys. Rep. **107**, 1 (1984).
- [3] S. V. Kravchenko and M. P. Sarachik, Rep. Prog. Phys. **67**, 1 (2004).
- [4] J. A. Chervenak and J. M. Valles, Phys. Rev. B **59**, 11209 (1999).

- [5] A. M. Goldman and N. Markovic, *Physics Today* **51**, 39 (1998).
- [6] N. Mason and A. Kapitulnik, *Phys. Rev. Lett.* **82**, 5341 (1999).
- [7] P. Phillips and D. Dalidovich, *Science* **302**, 243 (2003).
- [8] M. V. Feigel'man, A. I. Larkin, and M. A. Skvortsov, *Phys. Rev. Lett.* **86**, 1869 (2001).
- [9] B. Spivak, A. Zyuzin, and M. Hruska, *Phys. Rev. B* **64**, 132502 (2001).
- [10] P. M. Ostrovsky, M. A. Skvortsov, and M. V. Feigel'man, *JETP Lett.* **75**, 336 (2002).
- [11] J. A. Melsen *et al.*, *Europhys. Lett.* **35**, 7 (1996).
- [12] A. Lodder and Y. V. Nazarov, *Phys. Rev. B* **58**, 5783 (1998).
- [13] H. Schomerus and C. W. J. Beenakker, *Phys. Rev. Lett.* **82**, 2951 (1999).
- [14] T. Kouh and J. M. Valles, *Phys. Rev. B* **67**, 140506 (2003).
- [15] S. Y. Hsu *et al.*, *Physica B* **194**, 2337 (1994).
- [16] L. Merchant *et al.*, *Phys. Rev. B* **63**, 134508 (2001).
- [17] M. Tinkham, *Introduction to superconductivity* (The McGraw-Hill Companies, Inc., 1996).
- [18] L. N. Cooper, *Phys. Rev. Lett.* **6**, 689 (1961).
- [19] P. G. De Gennes, *Rev. Mod. Phys.* **36**, 225 (1964).
- [20] Y. V. Fominov and M. V. Feigel'man, *Phys. Rev. B* **63**, 094518 (2001).
- [21] O. Bourgeois, A. Frydman, and R. C. Dynes, *Phys. Rev. B* **68**, 092509 (2003).
- [22] A. K. Gupta *et al.*, *Phys. Rev. B* **69**, 104514 (2004).
- [23] K. D. Usadel, *Phys. Rev. Lett.* **25**, 507 (1970).
- [24] W. Belzig, C. Bruder, and G. Schon, *Phys. Rev. B* **54**, 9443 (1996).
- [25] N. Moussy, H. Courtois, and B. Pannetier, *Europhys. Lett.* **55**, 861 (2001).
- [26] S. Gueron *et al.*, *Phys. Rev. Lett.* **77**, 3025 (1996).
- [27] A. D. Truscott, R. C. Dynes, and L. F. Schneemeyer, *Phys. Rev. Lett.* **83**, 1014 (1999).
- [28] S. H. Tessmer *et al.*, *Phys. Rev. Lett.* **77**, 924 (1996).
- [29] K. L. Ekinci and J. M. Valles, *Phys. Rev. Lett.* **82**, 1518 (1999).
- [30] Z. Long and J. M. Valles (in preparation).
- [31] J. M. Valles, R. C. Dynes, and J. P. Garno, *Phys. Rev. Lett.* **69**, 3567 (1992).
- [32] S. Y. Hsu, J. A. Chervenak, and J. M. Valles, *Phys. Rev. Lett.* **75**, 132 (1995).
- [33] A. Bezryadin, C. N. Lau, and M. Tinkham, *Nature* **404**, 971 (2000).
- [34] S. Sachdev, P. Werner, and M. Troyer, *Phys. Rev. Lett.* **92**, 237003 (2004).
- [35] S. Tewari, *Phys. Rev. B* **69**, 014512 (2004).
- [36] The quasiparticle propagation in these granular bilayers is neither strictly ballistic nor strictly diffusive. It is generally believed that intragrain propagation is ballistic while the intergrain propagation is diffusive.
- [37] To ensure conservation of states for this form, we reduced N_G^s by the fraction of subgap states. This reduction made the peak heights on the left and right hand sides of Fig. 4a differ.